Statistical Analysis of the Roughness of Cortical Surfaces

Austin Rochford

1 Introduction

We are interested in investigating the roughness of the human cingulate gyrus, a region of the cortex of the brain. Ratnanather et al. [4] found that *local area*, a measure of surface roughness that they define, varies significantly between the cingulate gyri of control and schizophrenic subjects. We wish to statistically investigate the relationship between this new quantity, local area, and Gauss and mean curvature, two much more classical measures of surface roughness that have been well-studied and understood for more than a century (at least in the context of the human cingulate gyrus). We take much of our inspiration from the work of Ratnanather et al., so that our results may be applicable to their future research. We represent our cingulate gyri as triangulated surfaces, and the principle contribution of this research is the combined use of the theory of curvature measures on triangulated developed by Cohen-Steiner and Morvan [1] and Krummel and Zweck [2] and spatial averaging as developed in by Meyer et al. [3] to approximate the curvature of triangulated surfaces. Once we have computed our curvature approximations, we attempt to identify correlations between the curvature and local area of our sample cingulate gyri and analyze the significance of these correlations.

2 Local Area

Ratnanather et al. [4] define *local area* to quantify the roughness of a surface. Let $M \subseteq \mathbb{R}^3$ be a surface, and $p \in M$. Intuitively, the local area of M at p measures the amount of surface area of M that lies in a three dimensional ball centered at p. The radius of this ball is important to the definition of local area and is known as the *scale parameter*, σ. In practice, however, it is difficult to determine the intersection of a ball and a surface in $\mathbb{R}^3$, so Ratnanather et al. instead introduce a three dimensional Gaussian kernel centered at p to make computing local area more efficient. The scale parameter $\sigma > 0$ specifies the half-width of this Gaussian kernel, which is convolved with the area measure of M to define local area. This convolution causes the area of M close to p to contribute more to the local area at p.

Definition 1. Let $M \subseteq \mathbb{R}^3$ be a surface with $p \in M$ and $\sigma > 0$. The *local area* of M at p at the scale given by σ is

$$L_M(p,\sigma) = \int_M \exp\left(-\frac{1}{2}\left(\frac{\| p - x \|}{\sigma}\right)^2\right) dA(x). \tag{1}$$

Note that, as a measure of surface roughness, local area is defined using integration, whereas curvature, a more classical measure of surface roughness, is often defined using differentiation. In addition to local area, Ratnanather et al. define a quantity called the *magnitude of the relative local area*, which compares the local area of a surface to the local area of a plane at the same scale.

Definition 2. Let $M \subseteq \mathbb{R}^3$ be a surface with $p \in M$ and $\sigma > 0$. The *magnitude of the relative local area* of M at p at the scale given by σ is

$$l_M(p,\sigma) = \left|\frac{L_M(p,\sigma)}{2\pi\sigma^2} - 1\right|. \tag{2}$$

(Note that $2\pi\sigma^2$ is the local area of a plane at scale σ.)

3 Triangulated Surfaces

We call $T \subseteq \mathbb{R}^3$ a *triangulated surface* if it is a finite union of disjoint closed triangles. Each of these triangles is a *face* of T, their edges are the *edges* of T, and their vertices are the *vertices* of T. We say that T has no boundary, if each edge of T must belong to exactly two faces.

An *orientation* of a face is an ordering of its vertices. Note that a orientation on a face induces an orientation on each of its edges. As in the case of smooth surfaces, an orientation on a face defines a unit normal vector field over the face. In order for the unit normal vector field of T to be well defined, the orientations on adjacent faces must be compatible in the sense that the orientations induced on their common edge must be opposite, as illustrated in Figure 1. This compatibility of orientation is essential to obtaining accurate curvature estimates.

3.1 Data Acquisition

The data used in this study was provided by Prof. J. Cernansky at Washington University School of Medicine and Dr. J.T. Ratnanather at Johns Hopkins University. The process by which our cortical data is acquired necessitates our concern with triangulated surfaces. First, a subject underwent three MRI scans in quick succession. The three dimensional data from each of these scans was averaged in order to smooth any numerical artifacts introduced by the acquisition process. The marching cubes algorithm was then used to extract a triangulated isosurface that represents the cortex of the brain from this three dimensional

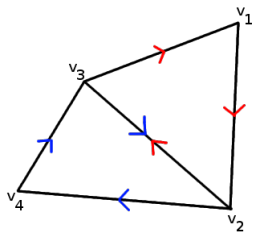

Figure 1: An example of compatible orientations on adjacent faces.

data. This isosurface then underwent further post-processing to isolate the cingulate gyrus, yielding the triangulated surfaces with which we work. The data used by Ratnanather et al. [4] was acquired in a similar process, except that only one MRI of the subject was used, so their data was not smoothed as much in pre-processing. We hope to obtain more accurate curvature estimates from our smoothed data.

3.2 Approximation of Local Area

Ratnanather et al. [4] not only define local area in the smooth case, but also give an approximation for triangulated surfaces. The key assumption that yields their approximation is that the scale of the triangles is sufficiently small so that the Gaussian kernel may be approximated by a constant over each one. Let $T \subseteq \mathbb{R}^3$ be a triangulated surface, with faces T_k for $k = 1, 2, \ldots, n$, with x_k the center of T_k. For $\sigma > 0$, Ratnanather et al. [4] use the approximation

$$L(x_i, \sigma) \approx \sum_{k=1}^{n} \exp\left(-\frac{\| x_i - x_k \|^2}{2\sigma^2}\right) \text{Area}(T_k). \tag{3}$$

We also use this approximation, computed with code provided by Ratnanather and his colleagues.

We extend the approximation in Equation 3 to the magnitude of the relative local area in the obvious fashion.

3.3 Approximation of Curvature

Many approximations of the curvatures of triangulated surfaces have been derived. We take the approach curvature measures on triangulated surfaces developed by Cohen-Steiner and Morvan [1] and Krummel and Zweck [2]. We adopt this approach for a number of reasons. The following logic shows that it is impossible to define curvature meaningfully on a triangulated surface. Consider any point on the surface. If the point is in the interior of a face, the surface as zero curvature at that point, since it is locally flat. If the point lies on an

edge, there is no clear choice of orientation at the point, and therefore we cannot differentiate the unit normal to obtain curvature in the classical manner of differential geometry. This difficulty that arises in attempting to define pointwise curvature on a triangulated surface naturally leads to the consideration of nonlocal approximations of curvature, most naturally curvature measures. In addition to its resolution of the above difficulty, there is a rich theory of curvature measures that has been developed in pure mathematics, and our approach can be regarded as an extension of this theory to applications involving triangulated surfaces.

Definition 3. Let $T \subseteq \mathbb{R}^3$ be a triangulated surface without boundary and let $B \subseteq \mathbb{R}^3$ be measurable. The *Gauss curvature measure* of T is given by

$$\phi_T^K(B) = \sum_{v \in B \cap T \text{ a vertex}} (2\pi - \theta(v)), \tag{4}$$

where $\theta(v)$ is the sum of the angles incident at v.

Definition 3 gives the Gauss curvature measure for triangulated surfaces defined by Cohen-Steiner and Morvan [1]. This curvature measure possesses several properties that make it both theoretically and computationally attractive. From a theoretical perspective, it measures the angle defect at each vertex, a concept intimately related to Gauss curvature in differential geometry. It also represents a discretization of the Local Gauss-Bonnet Theorem; it has been proved many times (for instance, in [2]) that $\phi_T^K(T) = 2\pi\chi(T)$, just as in the Global Gauss-Bonnet Theorem of smooth differential geometry. From a computational perspective, this measure is a linear combination of Dirac measures at each vertex of T, and is therefore simple to program and efficient to compute.

Definition 4. Let $T \subseteq \mathbb{R}^3$ be a triangulated surface without boundary and let $B \subseteq \mathbb{R}^3$ be measurable. The *mean curvature vector measure* of T is given by

$$\phi_T^{H\vec{U}}(B) = \sum_{e \subseteq B \cap T \text{ an edge}} -\sin\left(\frac{\beta_e}{2}\right) \text{length}(e \cap B)\, \vec{U}_e^+, \tag{5}$$

where β_e is the angle between the normal vectors of the two faces that contain e and $\vec{U}_e^+$ is the unit vector in the same direction as the sum of these two normals.

Figure 2 illustrates the geometry of the quantities β_e and $\vec{U}_e^+$. Krummel and Zweck [2] define the mean curvature vector measure, because, unlike its scalar counterpart, it is independent of the orientation on the triangulated surface. We use the magnitude of the mean curvature vector measure to approximate the absolute value of mean curvature. This measure is significantly more analytically complicated than the Gauss curvature measure, and is consequentially more difficult to program and more computationally expensive.

3.4 Spatial Averaging

Since we employ measures to approximate the curvature of triangulated surfaces, we obtain a total curvature (or curvature vector) for each subset of the surface.

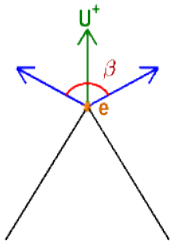

Figure 2: Two faces meeting, looking along their common edge.

In order to store our curvature estimates efficiently and compare them to the estimates of local area, we wish to obtain curvature estimates at the vertices of the triangulated surface. We reduce curvature estimates on a subset of the triangulated surface to estimates at a point on the surface by a process called *spatial averaging*. To each vertex of the triangulated surface, we associate a subset of the surface containing the vertex, and approximate the curvature at the vertex by dividing the value of the curvature measure on the set by the area of the set. Meyer et al. [3] define such a partitioning scheme that minimizes the error from this spatial averaging.

Given a vertex of the surface, this partitioning scheme considers its *one ring*, that is, all faces that contain the vertex. The set associated with the vertex will be a subset of the one ring of the vertex. For each face in the one ring, if the face is non-obtuse, it must contain its circumcenter. The portion of the associated set in that face is obtained by connecting its circumcenter with the midpoints of its two edges that contain the vertex; this region is commonly known as the *Voronoi region* of the triangle. The area of the Voronoi region of a non-obtuse triangle PQR is given by $A_{\text{Voronoi}} = \frac{1}{8}\left(|PR|^2 \cot \angle Q + |PQ|^2 \cot \angle R\right)$ [1]. If the face is obtuse, it cannot contain its circumcenter, so its Voronoi region will not lie completely within the one ring. In this case, if the angle of the face at the vertex is obtuse, the associated set contains half of the area of the face. If the angle of the face at the vertex is acute, the associated set contains one quarter of the area of the face. In both the obtuse and non-obtuse cases, it should be noted that the associated set meets the edges of the faces of the one ring at their midpoints. This special property simplifies the computation of the length term in Equation 5 and is illustrated in Figure 3. Another attractive property of this partitioning scheme, from a measure-theoretic perspective, is that for different vertices, the associated sets are disjoint, and the union of the sets for each of the vertices covers the surface. This property ensures that each point is counted exactly once during the spatial averaging process.

Through this spatial averaging we obtain estimates of curvature at each vertex of a triangulated surface which we can statistically compare to corresponding estimates of local area.

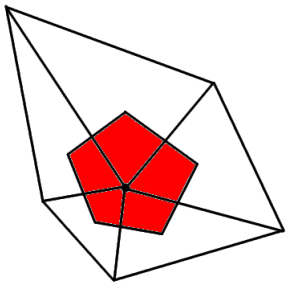

Figure 3: A vertex, its one ring, and the set used for spatial averaging (show in red).

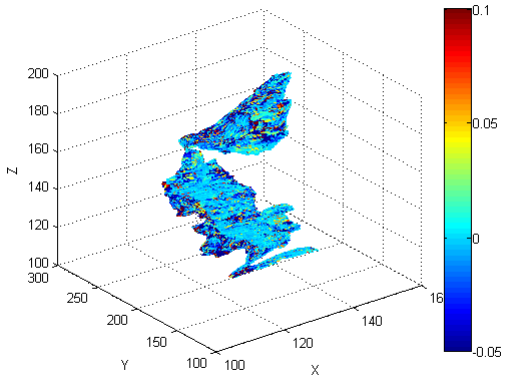

Figure 4: A right anterior cingulate gyrus colored by Gauss curvature.

4 Results and Analysis

4.1 Hypothesis

We use the approximations from the previous section to obtain estimates of curvature and local area for a set of cingulate gyri obtained via MRI. In order to formulate a hypothesis to be tested statistically, we plot these quantities on the triangulated surfaces they were obtained from as shown in Figure 4, Figure 5, and Figure 6.

The roughness of the coloring of these plots is due to the fine scales over which we take the local area and spatially average the curvature measures. These scales are on the order of the one rings of the vertices. We are motivated to use such a small scale (comparable to the scale of the one rings) by the results of Ratnanather et al. [4]. The relationship between surface roughness (as

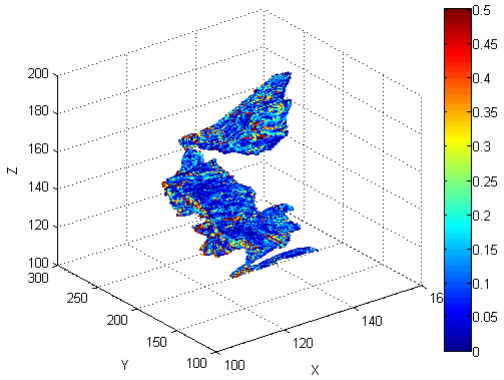

Figure 5: A right anterior cingulate gyrus colored by the absolute value of mean curvature.

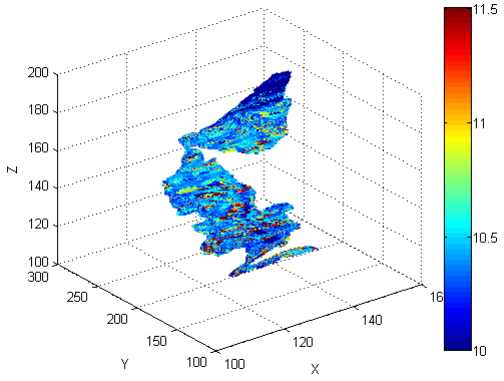

Figure 6: A right anterior cingulate gyrus colored by local area.

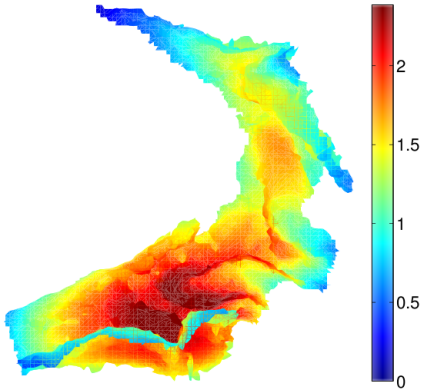

Figure 7: A cingulate gyrus colored by local area (obtained using a large scale).

measured by local area) and schizophrenia found in this research only occurs at fine scales approaching the scale of the triangulation. In order to obtain results applicable to this past research, we must investigate the relationship between curvature and local area at similar small scales. When we increase the scale of our local area estimates and our spatial averaging beyond the one ring of a vertex, the resulting plots become smoother. An example of such a smoother plot is shown for local area in Figure 7.

Our hypothesis concerns aggregate statistics from each sample cingulate gyrus. For each surface, we compute the mean, variation, first and second quantiles, and median of each of Gauss curvature, the absolute value of mean curvature, and local area, yielding fifteen statistics for each cortical surface. We then compare corresponding curvature and local area statistics in the following manner. We first choose a statistic to compare, for example, the median of Gauss curvature. We divide $\mathbb{R}^2$ into boxes, and for each sample cingulate gyrus, we plot the point whose coordinates are the median of Gauss curvature and the median of local area, and note in which box it falls. After repeating this procedure for each sample surface, we count the number of sample points in each box and assign each box a color and height based on this number. The results of this process are depicted in Figure 8 and Figure 9.

We observe in these two-dimensional histograms, particularly in Figure 9, that there appears to be a negative linear relationship between median Gauss curvature and median local area. That is, as median Gauss curvature increases, median local area decreases. This observed relationship and other similar ones present in the histograms of other statistics lead us to hypothesize that there is a linear relationship between each curvature statistic and the corresponding local area statistic.

We are most interested in the existence of a relationship between the medians of each curvature and local area. Of all five statistics computed, the median

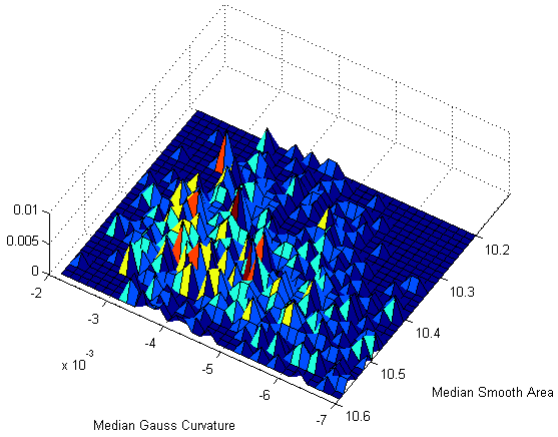

Figure 8: A two-dimensional histogram of median Gauss curvature vs. median local area with frequency indicated by color and height

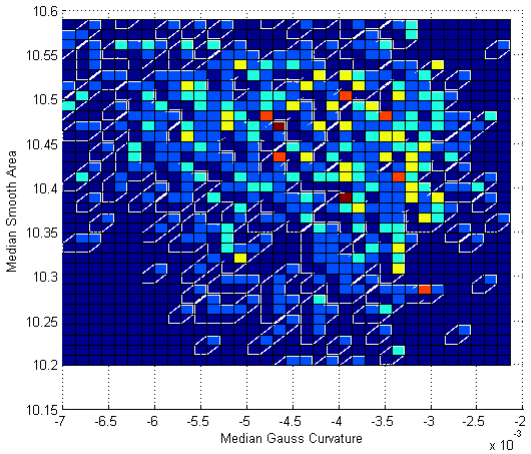

Figure 9: A two-dimensional histogram of median Gauss curvature vs. median local area with frequency indicated by color

is least sensitive to statistical outliers introduced that arise from numerical artifacts introduced during data acquisition process and the inherently fine scale of our approximations.

4.2 Correlation Coefficients

To test this hypothesis, we compute the *correlation coefficients* of various curvature and local area statistics.

Definition 5. Let X, Y be square-integrable random variables. The *correlation coefficient* of X and Y is

$$\rho_{X,Y} = \frac{\operatorname{Cov}(X,Y)}{\sigma_X \sigma_Y} = \frac{\operatorname{E}(XY) - \mu_X \mu_Y}{\sigma_X \sigma_Y}. \tag{6}$$

The correlation coefficient measures the extent of a linear relationship between two random variables. A correlation coefficient of one indicates a perfectly positive linear relationship, a correlation coefficient of zero indicates no linear relationship, and a correlation coefficient of negative one indicates a perfectly negative linear relationship. Note that the magnitude of the slope of the linear relationship is unimportant in relation to the correlation coefficient; only its sign matters. This is easily seen by computing the correlation of X and $Y = cX$ for $c \in \mathbb{R}$ ($\rho_{X,Y} = \operatorname{sgn}(c)$).

Definition 5, however, is only applicable to random variables whose distributions are known. In order to approximate this coefficient with samples from a population, we use the *sample correlation coefficient*.

Definition 6. Let X_k, Y_k be samples of two random variables for $k = 1, 2, \ldots, n$. The sample correlation coefficient of X and Y is

$$r_{X,Y} = \frac{1}{(n-1) S_X S_Y} \left(\sum_{k=1}^{n} X_k Y_k - n \bar{X} \bar{Y} \right), \tag{7}$$

where $\bar{X}$ and $\bar{Y}$ are the sample means of X and Y, and S_X and S_Y are their sample standard deviations.

Note the similarity between the second term in Equation 7 and the numerator in the second definition of the correlation coefficient in Equation 6.

An important consequence of making correlational inferences based on a sample of a population is that noise in the sample data may cause the correlation coefficient to be nonzero even when there is no linear relationship between the two random variables. In fact, the probability of the sample correlation coefficient being zero for any sample, correlated or not, is negligibly small. We therefore must test the correlation coefficients we compute for statistical significance. We use a two-tailed t-test to test for significance and decide to reject our hypothesis if its significance is less than .95.

Curvature	Mean	Variance	1^{st} quantile	Median	3^{rd} quantile
Gauss	0.051	0.024	-0.086	-0.25	-0.057
Abs. mean	0.32	0.12	0.036	0.26	0.51

Table 1: Correlation coefficients (with respect to corresponding statistic for local area)

Curvature	Mean	Variance	1^{st} quantile	Median	3^{rd} quantile
Gauss	0.79	0.45	0.97	≈ 1	≈ 1
Abs. mean	≈ 1	0.99	0.87	≈ 1	≈ 1

Table 2: Significance levels of the correlation coefficients in Table 1

4.3 Results

The sample correlation coefficients for each curvature statistic and the corresponding local area statistic are shown in Table 1.

While none of these coefficients indicate a perfectly linear relationship, several of them, most notably the median coefficients, are sufficiently different from zero to warrant investigation. When we test the significance levels of these correlation coefficients, we obtain the significance levels shown in Table 2. Table 2 shows that seven of the ten correlation coefficients are significant (that is, they exceed our significance threshold of .95). Note that we have only computed the significance levels to four significant digits, so a significance level of ≈ 1 is identical to 1 to four significant digits.

These significance levels confirm our hypothesis that there is a significant correlation between curvature and local area. We are particularly interested in the high (≈ 1) significance of the median correlations, as these were the statistics with which we were most concerned.

In Table 1 we are particularly interested in the negative correlation between Gauss curvature and local area. We hypothesize that as Gauss curvature increases, the surface locally resembles an increasingly curved paraboloid, causing the local area to decrease. In order to account for this type of relationship between Gauss curvature and local area, we consider a new set of statistics that measure the deviation of the local area of the cortical surfaces from the local area of a plane. This deviation is quantified by the magnitude of the relative local area. We repeat the statistical procedures detailed above, but instead of considering Gauss curvature, we consider the absolute value of Gauss curvature, and instead of considering local area, we consider the magnitude of the relative local area. The results of this analysis are shown in Table 3 and Table 4.

Curvature	Mean	Variance	1^{st} quantile	Median	3^{rd} quantile
Abs. gauss	0.040	0.034	0.050	0.172	0.402
Abs. mean	0.275	0.118	0.052	0.190	0.422

Table 3: Correlation coefficients (with respect to corresponding statistic for the magnitude of the relative local area)

Curvature	Mean	Variance	1^{st} quantile	Median	3^{rd} quantile
Abs. gauss	0.702	0.628	0.805	≈ 1	≈ 1
Abs. mean	≈ 1	0.998	0.827	≈ 1	≈ 1

Table 4: Significance levels of the correlation coefficients in Table 3

5 Conclusions

We are most interested in drawing conclusions from the data in Table 3 and Table 4, since the use of the magnitude of the relative area in the computation of these statistics allows use to compare the magnitude of curvature to the local differences between the surface and a plane. We see in Table 4 that the correlations between the medians of the absolute values of Gauss and mean curvature and the magnitude of the relative local area are highly correlated. We conclude that as curvature increases (in absolute value), the surface becomes increasingly less planar, as one would expect intuitively from the classical definition of curvature. This result provides new insight into the more recently developed local area of Ratnanather et al. [4] and its relationship to more classical measures of surface roughness (at least in the context of the cortical data that we have studied.)

References

[1] D. Cohen-Steiner and J.M. Morvan. Restricted delaunay triangulations and normal cycle. In *Symposium on Computational Geometry 2003*, pages 312–321. ACM, 2003.

[2] B. Krummel and J. Zweck. Curvature measures of triangulated surfaces with boundary. Preprint, 2007.

[3] M. Meyer, M. Desbrun, P. Schröder, and A.H. Barr. Discrete differential geometry operators for triangulated 2-manifolds.

[4] L. Younes, J. Zweck, L. Wang, M. Hosakere, J.T. Ratnanather, J. Csernansky, and M.I. Miller. Statistical analysis of surface roughness via local area maps: Application to the cingulate gyrus in healthy and schizophrenic subjects. In *2007 International Congress on Schizophrenia Research*, Colorado Springs, Colorado, 2007.